TISSUE ENGINEERING: Part A
Volume 16, Number 2, 2010

DOI: 10.1089/ten.tea.2009.0491

Rapid Anastomosis of Endothelial Progenitor Cell–Derived Vessels with Host Vasculature Is Promoted by a High Density of Cotransplanted Fibroblasts

Xiaofang Chen, Ph.D.,[1] Anna S. Aledia, B.S.,[1] Stephanie A. Popson, M.S.,[2] Linda Him, B.S.,[2] Christopher C.W. Hughes, Ph.D.,[1–3,*] and Steven C. George, M.D., Ph.D.[1,3,4,*]

To ensure survival of engineered implantable tissues thicker than approximately 2–3 mm, convection of nutrients and waste products to enhance the rate of transport will be required. Creating a network of vessels *in vitro*, before implantation (prevascularization), is one potential strategy to achieve this aim. In this study, we developed three-dimensional engineered vessel networks *in vitro* by coculture of endothelial cells (ECs) and fibroblasts in a fibrin gel for 7 days. Vessels formed by cord blood endothelial progenitor cell–derived ECs (EPC-ECs) in the presence of a high density of fibroblasts created an interconnected tubular network within 4 days, compared with 5–7 days in the presence of a low density of fibroblasts. Vessels derived from human umbilical vein ECs (HUVECs) *in vitro* showed similar kinetics. Implantation of the prevascularized tissues into immune-compromised mice, however, revealed a dramatic difference in the ability of EPC-ECs and HUVECs to form anastomoses with the host vasculature. Vascular beds derived from EPC-ECs were perfused within 1 day of implantation, whereas no HUVEC vessels were perfused at day 1. Further, while almost 90% of EPC-EC–derived vascular beds were perfused at day 3, only one-third of HUVEC-derived vascular beds were perfused. In both cases, a high density of fibroblasts accelerated anastomosis by 2–3 days. We conclude that both EPC-ECs and a high density of fibroblasts significantly accelerate the rate of functional anastomosis, and that prevascularizing an engineered tissue may be an effective strategy to enhance convective transport of nutrients *in vivo*.

Introduction

Tissue engineering promises treatment for a wide range of diseases caused by tissue damage or dysfunction.[1,2] One critical obstacle in this promising field is vascularization of the engineered tissues. The most successful applications of tissue engineering to date have been limited to thin (<2 mm) avascular tissues, such as skin[3] and cartilage,[4] in which delivery of nutrients and oxygen occurs by diffusion. Before the establishment of blood flow, cells in the inner portion of an implanted tissue are exposed to an environment with minimal oxygen and nutrients, which can lead to significant cell death.[5,6] The *in vitro* formation of mature vessel networks ready to anastomose with the host vasculature shortly after implantation has the potential to dramatically improve the rate of oxygen and nutrient delivery and waste product removal, and thus increases the viability of larger implanted tissues.[7–10] Clearly, the rates of anastomosis and perfusion of implantable tissues are critical parameters. Rapid (~1 day) anastomosis of the engineered vessels with host vasculature is likely necessary for the survival and function of tissue-specific cells, especially for oxygen-sensitive cells such as cardiomyocytes, hepatocytes, and stem cells, all of which are of tremendous interest in the field of regenerative medicine.

The source of endothelial cells (ECs) to create the vascular network is a critical issue. The cells should be clinically available, easy to purify and expand *in vitro*, and, ideally, autologous, thus avoiding host immune responses. Generation of functional vessels *in vivo* has been reported using mature ECs such as human umbilical vein ECs (HUVECs)[11,12] and human dermal microvascular ECs.[13] However, either these cells are unavailable for adults, or they require an invasive procedure to harvest. Human embryonic stem cells (hESCs) are pluripotent and can differentiate into all human cell types. The use of hESC-derived ECs in regenerative medicine has also been reported.[14,15] However, hESCs face the potential problem of sourcing and host immune rejection.[16] Alternatively, there is significant evidence demonstrating the angiogenic potential

Departments of [1]Biomedical Engineering and [2]Molecular Biology and Biochemistry, [3]The Edwards Lifesciences Center for Advanced Cardiovascular Technology, and [4]Department of Chemical Engineering and Material Science, University of California, Irvine, Irvine, California.
*These two authors contributed equally to this work.

of endothelial progenitor cells (EPCs), including those of adult origin.[17–19] Although a rigorous accounting of the origins of EPCs is still to be defined,[20] the presence of EPCs in human peripheral blood makes them an attractive cell type in regenerative cell therapies, especially as the collection of autologous cells from patients' peripheral blood is a viable procedure. For example, transplanted EPCs have been shown to induce angiogenesis and restore the function of ischemic tissue.[21,22] Importantly, like other ECs, EPCs can form robust vessel networks in engineered tissue constructs in the presence of stromal cells, and can be functional *in vivo* for up to 28 days.[17–19] However, a study addressing the critical issue of the rate of anastomosis using engineered vessels formed by EPCs has yet to be reported.

We demonstrated in our previous study that prevascularization of engineered tissue constructs with well-formed HUVEC vessel networks accelerated the formation of functional anastomosis (by day 7 in thin tissues) and enhanced the metabolic activity of implanted cells.[23] The objective of our current study was to significantly accelerate the anatomosis of the implanted vessel network by using EPCs and manipulating stromal cell density. We demonstrate that tissues developed for 7 days *in vitro* with ECs derived from EPCs and a high density of fibroblasts are more mature (as evidenced by enhanced association of α-smooth muscle actin [α-SMA]–positive cells with the capillaries) and anastomose with the host circulation as early as 1 day (27 h) postimplantation. Our study is the first to create mature *in vitro* vessel networks that anastomose with host vessels within this rapid time frame. Our prevascularization model has potential applications in tissue engineering and regenerative medicine.

Materials and Methods

Isolation of EPC-ECs from cord blood

Human umbilical cord blood was obtained from the University of California–Irvine Medical Center according to an Institutional Review Board–approved protocol. EPC-ECs were isolated as previously described.[24] Briefly, mononuclear cells were separated from 15 to 20 mL cord blood using a lymphocyte separation medium (Fisher Scientific, Pittsburgh, PA). The mononuclear cells were then seeded on 1% gelatin (Sigma, St. Louis, MO)–coated tissue culture flasks and fed with a 1:1 mixture of EGM-2 and M199 (Invitrogen, Carlsbad, CA), supplemented with 20% fetal bovine serum and 1% Endothelial Cell Growth Supplements (Fisher Scientific) for 2–4 weeks. The endothelial outgrowth cells were purified using CD31 (Dako, Carpinteria, CA)–coated magnetic beads (New England Biolabs, Ipswich, MA) and referred to as EPC-ECs. Once confluent, cultures were split 1:3 every 2–3 days. Passage 3–5 EPC-ECs were used in all experiments. HUVECs were isolated as previously described,[25,26] and were utilized at passage 3.

Characterization of HUVECs and EPC-ECs

Flow cytometric analyses of HUVECs and EPC-ECs were carried out by labeling the cells with Alexa Fluor 488–conjugated mouse anti-human CD45 (Invitrogen) diluted at 1:20 and fluorescein isothiocyanate–conjugated mouse anti-human CD90 (BioLegend, San Diego, CA) diluted at 1:5. Surface expression of CD31 was determined by immunostaining the cells with mouse anti-human CD31 (Dako) diluted at 1:25, followed by fluorescein isothiocyanate–conjugated goat anti-mouse secondary antibody (Jackson ImmunoResearch, West Grove, PA) diluted at 1:50. Isotype control antibody (Santa Cruz Biotechnology, Santa Cruz, CA) without dilution was used as a negative control. Antibody labeling was carried out for 20 min on ice followed by two washes in phosphate-buffered saline with 1% bovine serum albumin and resuspension in 2% paraformaldehyde. Cells were subsequently characterized using a FACS Calibur flow cytometer and CellQuest Software (Becton Dickinson, Franklin Lakes, NJ).

Morphology of HUVECs and EPC-ECs were compared in two-dimensional cultures with or without fibroblasts. HUVECs and EPC-ECs were seeded in 12-well plates for 24 h to allow the cells to attach. Then, Transwells® seeded with a monolayer of fibroblasts were inserted into the wells with HUVECs or EPC-ECs. Phase contrast images of HUVECs and EPC-ECs were taken 3 days after coculture with the fibroblasts with an Olympus IX51 microscope (Olympus America, Center Valley, PA).

Assembling of three-dimensional prevascularized tissue constructs

The prevascularized tissue constructs were prepared as previously described.[23] ECs and fibroblasts were suspended in a 10 mg/mL fibrinogen solution. The cell solutions were then mixed with thrombin at a concentration of 2 units/mL. The density of ECs was kept constant at 1 million/mL, while the density of fibroblasts ranged from 0.2 to 2 million/mL. The tissue constructs were cultured *in vitro* for 7 days in EGM-2 before implantation.

Immunofluorescent staining of whole tissue

To observe the vessel networks formed by ECs, some of the *in vitro* tissue constructs were immunofluorescently stained with anti-human CD31 antibody at 2, 4, and 7 days after the initial creation. The tissues were first fixed in 10% neutral-buffered formalin for 10 min, followed by permeabilization with 0.5% tris buffered saline with 0.1% Tween (TBST) for 15 min. The tissues were then blocked with 2% bovine serum albumin for 1 h followed by overnight incubation with a mouse anti-human CD31 antibody (Dako), which was diluted 1:200. Alexa Fluor 488–conjugated Goat anti-mouse IgG (Invitrogen) diluted at 1:500 was then applied to the tissues and incubated overnight to observe the ECs. Images of the stained vessels were taken using a Zeiss LSM 510 Meta laser scanning confocal microscope (Zeiss, Jena, Germany). For each condition, 10 images were taken randomly with the 10× objective. Total vessel length/mm^2, total number of continuous vessel networks/mm^2, average length of vessel network, and average number of branches/vessel network were quantified as previously described.[23]

Implantation of the prevascularized tissue constructs

Tissues were made in small polydimethysiloxane (PDMS) wells and transplanted subcutaneously within the wells on the dorsal area of ICR-SCID (Taconic Farms, Oxnard, CA)

mice as previously described.[23] The internal dimensions of the PDMS were 2 mm in height and 10 mm in diameter. In this geometry, delivery of nutrients was limited to only one surface making the effective thickness of the tissue 4 mm. The implanted tissues and PDMS wells were then harvested at days 1, 2, 3, and 5. Animal surgeries and animal handling were performed according to National Institutes of Health guidelines for laboratory animal usage, under a protocol approved by the Institutional Animal Care and Use Committee at the University of California, Irvine.

Immunohistochemical and immunofluorescent staining of tissues

Immunohistochemical and immunofluorescent staining were performed on 5 μm formalin-fixed, paraffin-embedded tissue sections. After deparaffinization and rehydration, epitope was recovered using the Target Retrieval solution (Dako) at 98°C for 20 min. Immunohistochemical staining was performed using the Dako Envision HRP-DAB system (Dako). Tissue sections were incubated with mouse anti-human CD31 antibody diluted at 1:200 or mouse anti-human α-SMA antibody diluted at 1:800 overnight, followed by labeling with the horseradish peroxidase–conjugated anti-mouse secondary antibody for 30 min. The sections were counterstained with hematoxylin alone or hematoxylin and eosin. Vessels positively stained with anti-human CD31, and with red blood cells in the lumen were considered perfused vessels.

For immunofluorescent staining, tissue sections were incubated with primary antibodies for 2 h, after 1-h blocking with 2% bovine serum albumin. The dilutions were 1:400 for the rabbit anti-human von Willebrand factor antibody (Dako) and 1:800 for the mouse anti-human α-SMA. Alexa Fluor 488–labeled goat anti-mouse and Alexa Fluor 555–conjugated goat anti-rabbit immunoglobin (Invitrogen) were used as the secondary antibodies (1:500 dilution) and were applied for 30 min. For double staining of von Willebrand factor and α-SMA, antibodies were added sequentially with an additional 1-h blocking performed before addition of the second antibody.

Statistics

All quantifications were performed by three researchers blinded to the conditions. The results are reported as mean ± standard deviation. For variables with significant differences among the groups (analysis of variance), paired comparisons (Student's *t*-test) were applied with Bonferroni's multiple comparison adjustment. Results were considered statistically significant when $p < 0.05$.

Results

Characterization of EPC-ECs and HUVECs

EPC-ECs were isolated by selection of CD31-positive cells from cord blood mononuclear cells as previously described. It was previously reported that cells isolated using this method demonstrated an endothelial phenotype and developed into functional vessel networks after implantation.[24] The hematopoietic marker CD45 and the mesenchymal marker CD90 were not detected by the flow cytometric characterization (Fig. 1A, D), excluding the possibility of contamination by hematopoietic or mesenchymal cells. Based on the isolation methods and the previous phenotypic characterization results, the endothelial outgrowth separated from cord blood mononuclear cell culture with the CD31 antibody was referred to as EPC-ECs. Interestingly, the EPC-ECs expressed considerably higher levels of CD31 than HUVECs (Fig. 1A, D), suggesting that they are a distinct population of ECs.

We then characterized the EPC-ECs in two-dimensional cell culture (Fig. 1). EPC-ECs showed a typical cobblestone-like morphology (Fig. 1E), but were smaller than HUVECs (Fig. 1B). EPC-ECs also proliferated more rapidly, with a doubling

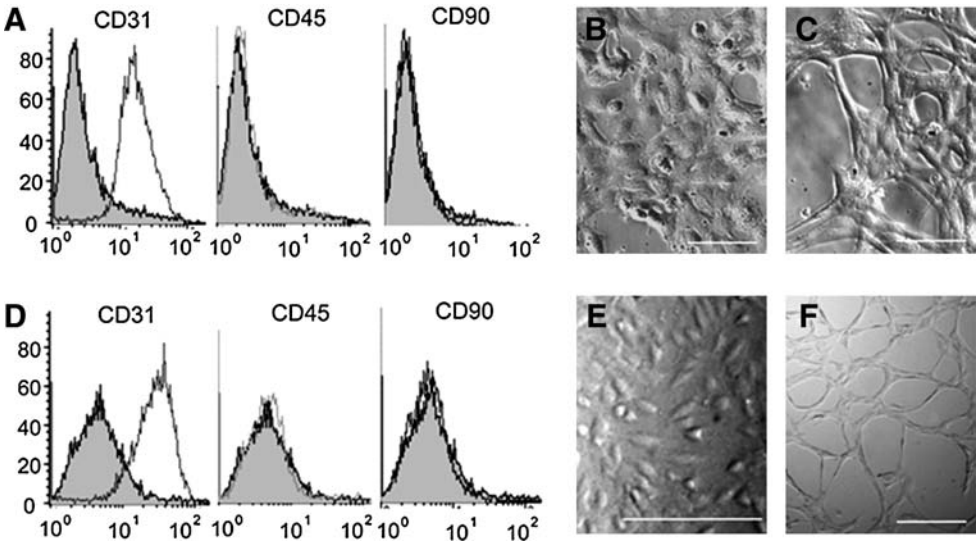

FIG. 1. Characterization of HUVECs and EPC-ECs by flow cytometry and two-dimensional cell culture. Flow cytometric analysis of (**A**) HUVECs and (**D**) EPC-ECs for CD31, CD45, and CD90. White area (histogram) represents cells stained with specific fluorescent antibody. Gray area (histogram) represents isotype matched control cells. Brightfield images of (**B**) HUVECs and (**E**) EPC-ECs in two-dimensional culture. Morphology of (**C**) HUVECs and (**F**) EPC-ECs after coculture with fibroblasts in Transwell plates. The HUVECs and EPC-ECs were plated as a two-dimensional monolayer culture. EPC-ECs elongated and formed homogeneous networks, demonstrating a significant morphological change. In contrast, the phenotypic change of HUVECs is heterogeneous with a less well-developed network. Scale bars represent 50 μm. HUVECs, human umbilical vein endothelial cells; EPC-ECs, endothelial progenitor cell–derived endothelial cells.

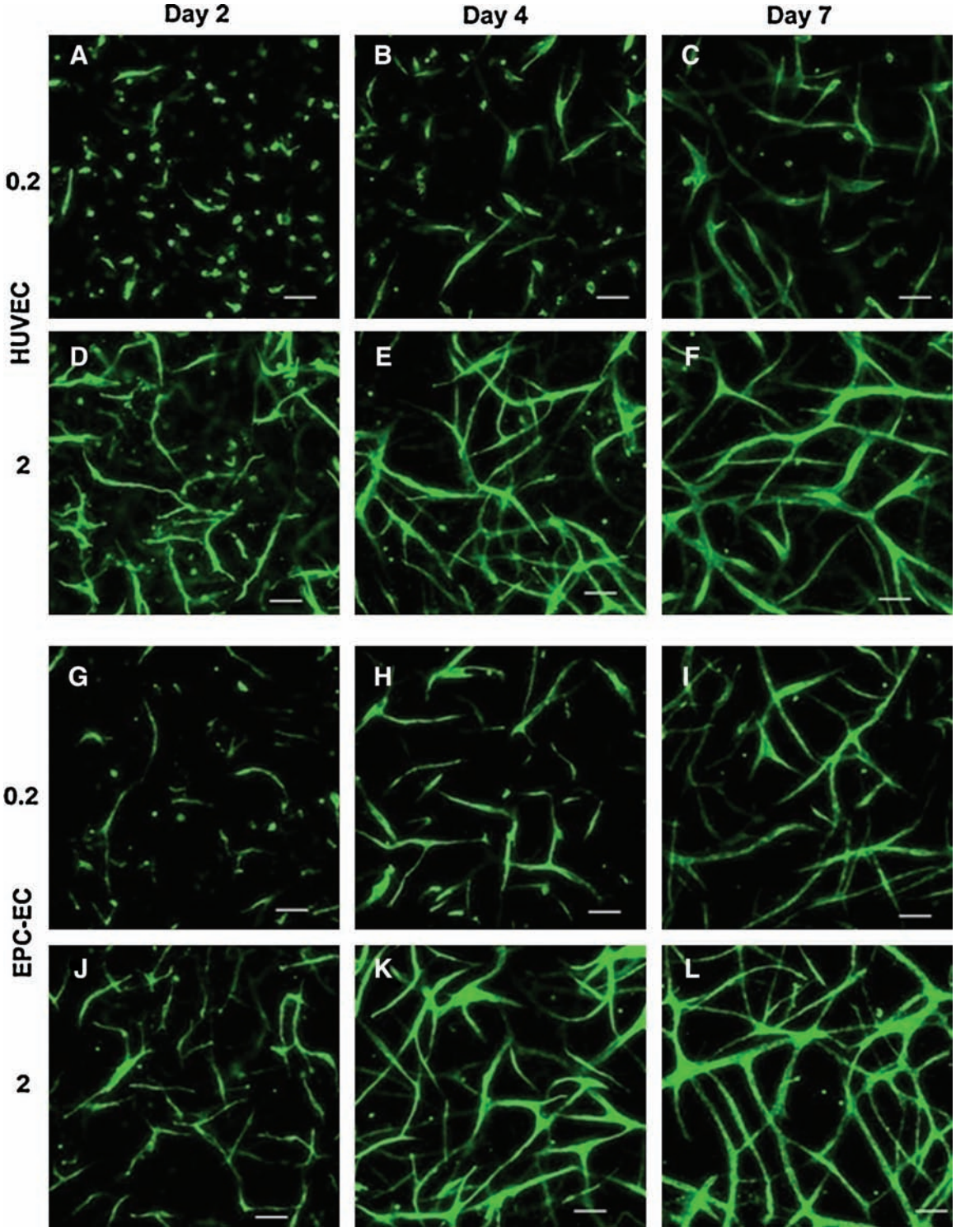

FIG. 2. Three-dimensional interconnected vessel networks form within 7 days *in vitro*. (**A–F**) HUVECs or (**G–L**) EPC-ECs were cocultured with fibroblasts in a three-dimensional fibrin gel. Endothelial cells were observed with an anti-human CD31 antibody. Vessel networks developed faster with a high density of fibroblasts (2 million cells/mL, **D–F**, **J–L**) and EPC-ECs compared with a low density of fibroblasts (0.2 million cells/mL, **A–C**, **G–I**) and HUVECs. Scale bars represent 50 μm. Color images available online at www.liebertonline.com/ten.

time of approximately 1 day for passage 4 cells compared with 2 days for passage 2 HUVECs. Remarkably, when fibroblasts growing in a Transwell were added to the cultures, the EPC-ECs demonstrated a dramatic change in morphology with the cells rearranging to form two-dimensional networks (Fig. 1F). In contrast, the change in morphology of HUVECs was not so dramatic, and more heterogeneous (Fig. 1C), with some of the cells still flattened in the morphology of the monolayer sheets. The differential response of EPC-ECs and HUVECs to the addition of fibroblasts led us to hypothesize that the cells

might behave differently in three-dimensional cultures *in vitro* and when transplanted *in vivo*.

In vitro *vessel networks*

Figures 2 and 3 present qualitative and quantitative features of the *in vitro* vessel networks. Both EPC-ECs and HUVECs formed interconnected vessel networks *in vitro* (Fig. 2) in response to fibroblast-derived factors,[27] and vessel formation was more pronounced at the higher density of fibroblasts. Specifically, ECs started to form elongated tubes at day 2 with a high density of fibroblasts (Fig. 2D, J), whereas most of the ECs still displayed a spherical morphology at day 2 with a low density of fibroblasts (Fig. 2A, G). In addition, by day 2 branched vessel networks were formed in tissues with a high density of fibroblasts (Fig. 2E, K). In contrast, only single, nonbranched endothelial tubes were observed in the tissue constructs with a low density of fibroblasts (Fig. 2A, G). By day 4 the vessel networks with a high density of fibroblasts were more developed (Fig. 2B, E, H, K), and by day 7, continuous vessel networks occupying an extended area were observable, and again, these were considerably more pronounced in the high fibroblast density cultures.

The impact of EPC-ECs compared with HUVECs as the EC source is less obvious from the qualitative images. However, after quantification of the vessel networks (Fig. 3), distinct trends can be observed. At day 4, the total lengths of EPC-EC vessels with low or high densities of fibroblasts were both more than 50% longer than vessels formed by HUVECs. At day 7, total vessel length, average length, and average number of branches per vessel network are all significantly higher in vessels formed by EPC-ECs than in vessels formed by HUVECs, regardless of the density of fibroblasts. The number of networks also decreased as multiple smaller networks coalesced.

In vivo *anastomosis*

Figure 4 presents histological images (hematoxylin and eosin stain) as well as the gross appearance (inset) of the tissues 1, 2, 3, and 5 days after implantation and subsequent harvest. By day 5, all tissues regardless of endothelial source or density of fibroblasts demonstrated some degree of anastomosis and perfusion of the implanted tissue. However, tissues with a higher density of fibroblasts were perfused earlier, and tissues with vessel networks derived from EPC-ECs anastomosed with host vessels earlier than vessels formed by HUVECs. These observations are consistent with the trends observed for *in vitro* vessel development.

Vessels formed by EPC-ECs in the presence of 2 million fibroblasts/mL were perfused with mouse blood as early as day 1 (27 h, Fig. 4M), whereas HUVEC-lined vessels were perfused no earlier than day 3 (Fig. 4G). In contrast, red blood cells first appeared in the vessels with a low density of fibroblasts at later time points (day 3 for EPC-ECs, Fig. 4K; day 5 for HUVECs, Fig. 4D). Consistent with the histology, macroscopic images (Fig. 4 insets) also indicate perfusion of the implanted tissues by host blood, with the perfused tissues appearing partially or completely red, while unperfused tissue constructs were white and transparent.

Table 1 summarizes the number of perfused tissue constructs relative to the total number of implanted tissue constructs at different time points. At both days 1 and 2, about

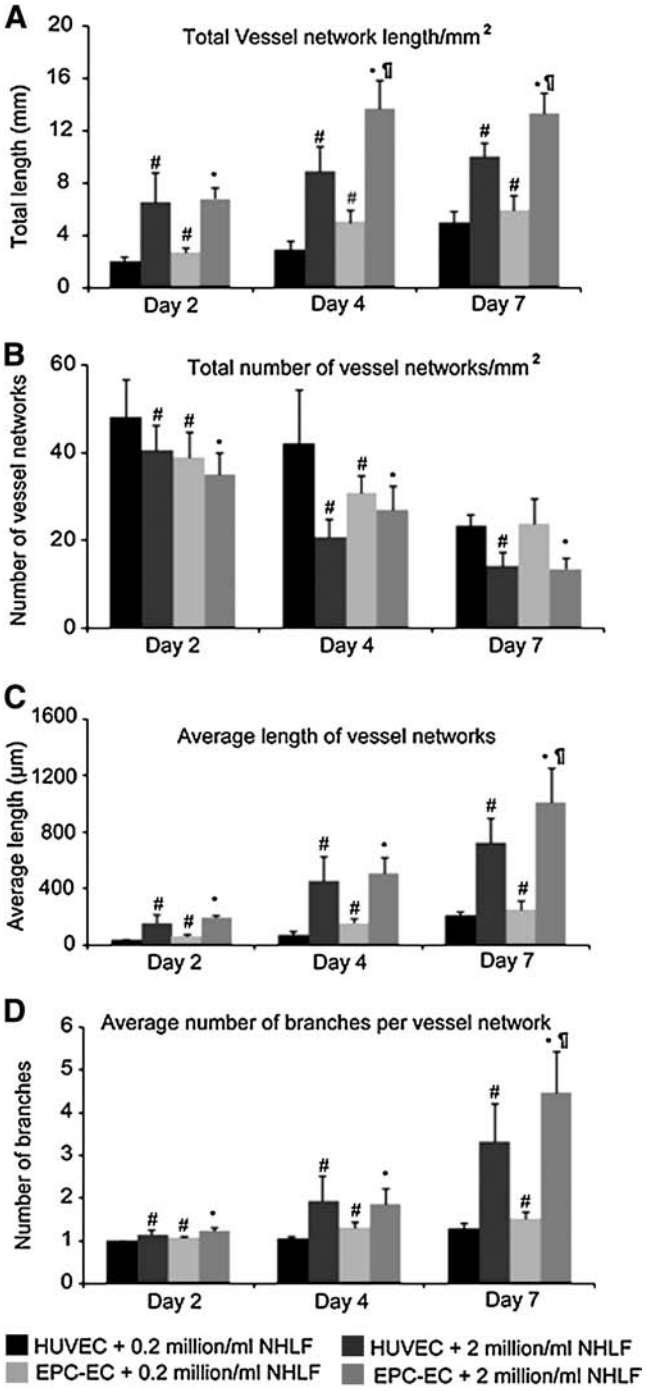

FIG. 3. Quantification of three-dimensional *in vitro* vessel networks. (**A**) Total vessel length, (**C**) average length of vessel networks, and (**D**) number of branches per network significantly increase in the presence of a high density of fibroblasts, whereas (**B**) the total number of vessel networks decreases as smaller networks coalesce. At day 7, total vessel length, average network length, and average number of branches all peaked in tissue constructs comprised of EPC-ECs with 2 million cells/mL fibroblasts. #Significantly different from HUVECs with 0.2 million cells/mL fibroblasts. *Significantly different from EPC-ECs with 0.2 million cells/mL fibroblasts. ¶Significantly different from HUVECs with 2 million cells/mL fibroblasts. $p < 0.05$.

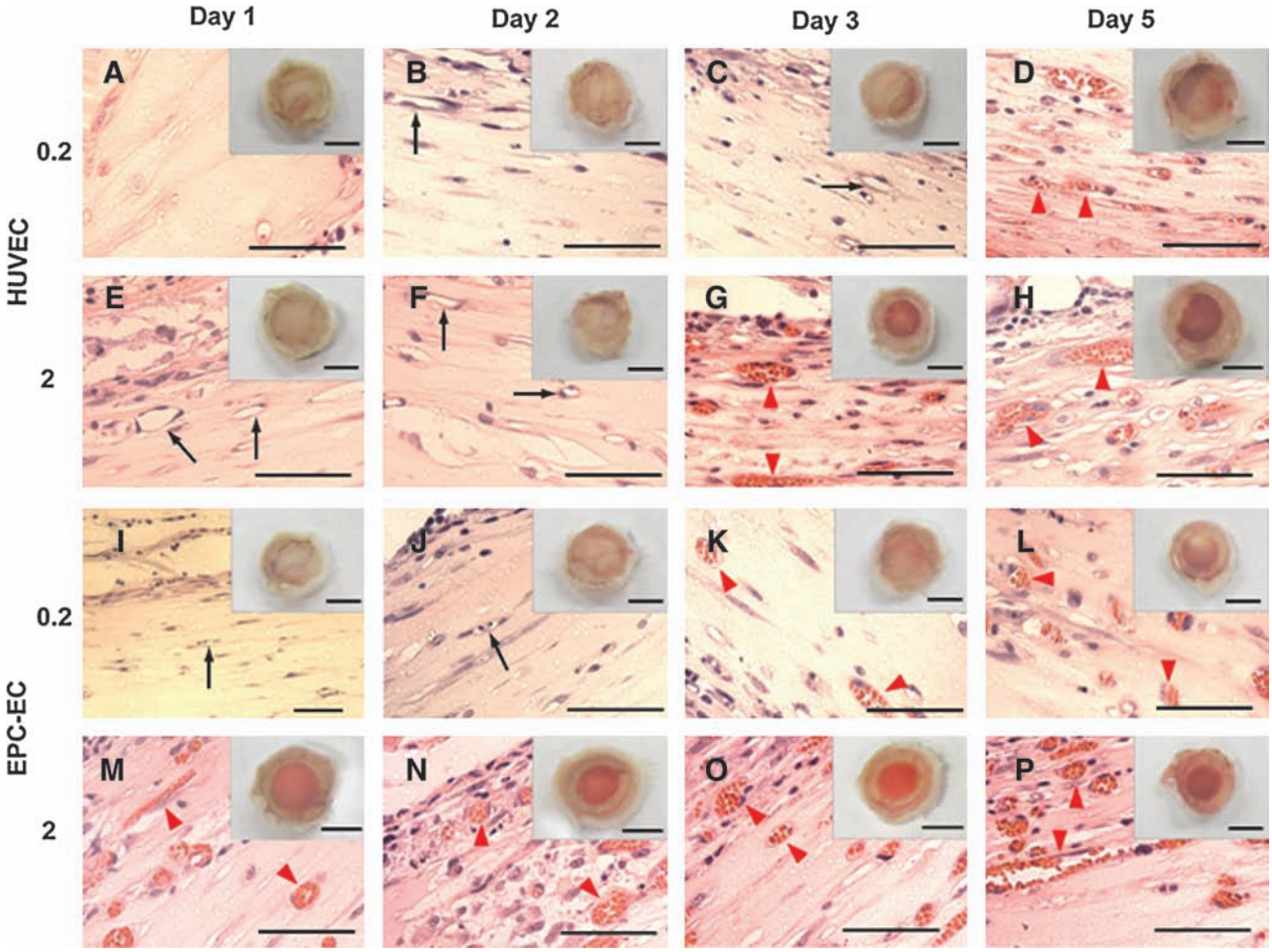

FIG. 4. Tissue constructs prevascularized with vessels formed from EPC-ECs in the presence of a high density of fibroblasts rapidly anastomose with host vasculature are perfused within 1 day postimplantation. (**A–P**) Hematoxylin and eosin stain of implanted tissues constructs harvested at days 1, 2, 3, and 5. Insets, macroscopic view of the tissue constructs postimplant. (**D**) Vessels formed by HUVECs with 0.2 million cells/mL fibroblasts demonstrate anastomosis with mouse vasculature 5 days postimplant. (**G**) With 2 million cells/mL fibroblasts, HUVEC vessels anastomose with host vasculature at day 3. Mouse red blood cells are observed in the vessels formed by EPC-ECs at 1 day (**M,** 2 million cells/mL fibroblast) or 3 days (**K,** 0.2 million cells/mL fibroblast) postimplantation. Black arrows indicate unperfused lumens surrounded by endothelial cells. Red arrowheads indicate vessels perfused by mouse blood. Scale bars represent 50 μm in (**A–P**) and 5 mm in insets.

29% (two out of seven) of the tissues comprised of EPC-ECs and a high density of fibroblasts were perfused with mouse blood, while none of the other tissue types were perfused. One of the perfused tissue constructs at day 1 and both of the perfused tissues at day 2 were completely red (Fig. 4M inset), consistent with perfusion throughout the tissue construct. At day 3, most of the EPC-EC vascular beds with a high density of fibroblasts (six out of seven, 86%) were perfused, compared with 33% with a low density of fibroblasts. In addition, 33% of the HUVEC vascular beds with 2 million/mL fibroblasts were also perfused. At day 5, blood cells were seen in one-third of the tissues comprised of HUVECs and 0.2 million/mL fibroblasts. All of the other types of tissues were perfused with mouse blood at day 5.

Table 1. Summary of the Percentage of Implanted Tissue Constructs Perfused by Host Blood

EC type	*Fibroblasts (millions/mL)*	*Day 1*	*Day 2*	*Day 3*	*Day 5*
HUVECs	0.2	0/6 (0)	0/6 (0)	0/11 (0)	3/9 (33%)
HUVECs	2	0/6 (0)	0/6 (0)	2/11 (18%)	8/8 (100%)
EPC-Ecs	0.2	0/3 (0)	0/3 (0)	2/6 (33%)	3/3 (100%)
EPC-Ecs	2	2/7 (29%)	2/7 (29%)	6/7 (86%)	4/4 (100%)

ECs, endothelial cells; HUVECs, human umbilical vein endothelial cells; EPC-ECs, endothelial progenitor cell–derived endothelial cells.

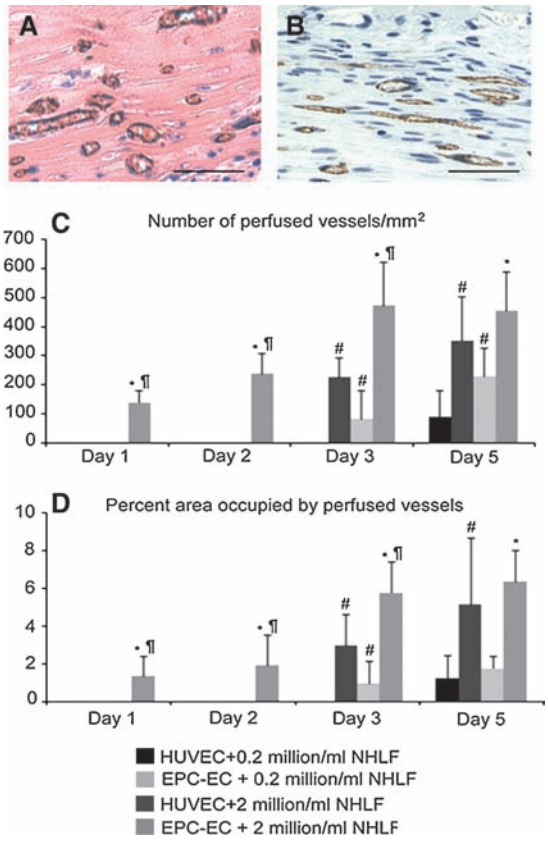

FIG. 5. Quantification of perfused vessels formed by HUVECs and EPC-ECs. Perfused vessels formed by (**A**) EPC-ECs and (**B**) HUVECs in the implanted tissue constructs are of human cell origin as evidenced by staining with anti-human CD31 (black staining) and counterstained with hematoxylin and eosin (**A**) or hematoxylin alone (**B**). The number of perfused vessels (**C**) and area fraction occupied by perfused vessels (**D**) both peak in tissue constructs comprised of EPC-ECs with 2 million cells/mL fibroblasts. #Significantly different from HUVECs with 0.2 million cells/mL fibroblasts. *Significantly different from EPC-ECs with 0.2 million cells/mL fibroblasts. ¶Significantly different from HUVECs with 2 million cells/mL fibroblasts. $p < 0.05$.

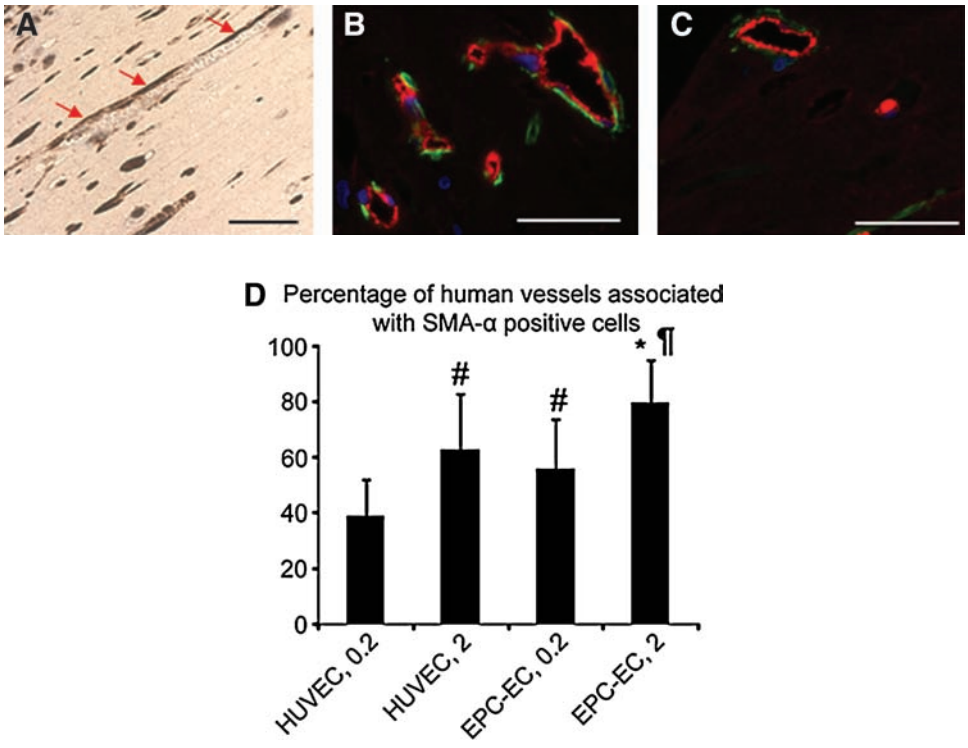

FIG. 6. A larger fraction of vessels formed by EPC-ECs associate with α-SMA–positive cells. (**A**) Immunohistochemical stain of the tissue demonstrates presence of numerous α-SMA–positive cells (brown) 1 day postimplantation. Red arrows highlight α-SMA–positive cells lining a vessel filled with red blood cells. Costain of the section with anti-human von Willebrand factor and α-SMA shows that α-SMA–positive cells closely associate and wrap around the vessels formed by (**B**) EPC-ECs and (**C**) HUVECs. (**D**) Quantification of the vessels 1 day postimplantation demonstrates that approximately 80% of the vessels formed by EPC-ECs with 2 million cells/mL fibroblasts were associated with α-SMA–positive cells, significantly higher than vessels formed by HUVECs or lower density of fibroblasts. #Significantly different from HUVECs with 0.2 million cells/mL fibroblasts. *Significantly different from EPC-ECs with 0.2 million cells/mL fibroblasts. ¶Significantly different from HUVECs with 2 million cells/mL fibroblasts. $p < 0.05$. Scale bars represent 50 μm. α-SMA, α-smooth muscle actin.

Immunohistochemical staining with anti-human CD31 (Fig. 5A, B) demonstrated that the perfused vessels in the implanted tissue constructs were lined by human ECs, consistent with functional anastomosis of the preformed vessel networks with mouse vasculature. Quantification of the perfused vessels demonstrated a significantly higher number of perfused vessels in the tissue constructs comprised of a high density of fibroblasts (Fig. 5C). The same trends were seen in the percent area occupied by perfused vessels (Fig. 5D). Both indices peaked in tissue constructs prevascularized by EPC-ECs and a high density of fibroblasts, a trend consistent with the *in vitro* vessel network development (Figs. 2 and 3) and the rate of *in vivo* anastomosis (Fig. 4).

Higher percentage of vessels formed by EPC-ECs are associated with α-SMA–positive cells

To probe the mechanism of early and more extensive anastomosis and perfusion of vessels formed by EPC-ECs, the tissue constructs harvested at day 1 postimplant were stained for α-SMA, a phenotypic marker of myofibroblasts or pericytes. Figure 6 demonstrates that α-SMA–positive cells wrap around vessels (ECs identified by the presence of von Willebrand factor) formed by both HUVECs and EPC-ECs, consistent with the behavior of pericytes. For both HUVEC-derived and EPC-EC–derived vessel networks, the percentage of vessels wrapped by α-SMA–positive cells was significantly higher in tissue constructs seeded with a high density of fibroblasts compared with tissues with a low density (Fig. 6D). Further, for both high and low density fibroblast tissue constructs, a significantly higher percentage of vessels formed by EPC-ECs were associated with α-SMA–positive cells.

Discussion

In this study, we compared the *in vitro* and *in vivo* angiogenic potential of EPC-ECs to HUVECs in three-dimensional tissue constructs coseeded with a low and high density of fibroblasts. All of our *in vitro* and *in vivo* endpoints demonstrated superior performance of EPC-ECs compared with HUVECs, and high density fibroblast tissue constructs compared with low density. Of particular interest is our observation of anastomosis and perfusion as early as 1 day (27 h) postimplant in tissue constructs prevascularized with vessel networks derived from EPC-ECs with a high density of fibroblasts. Our study is the first to achieve blood perfusion in an engineered tissue construct within this time frame. The rapid perfusion of the implanted vessels by host blood suggests that our model of prevascularizing an implantable tissue with a mature interconnected network of capillaries has applications in the creation of tissues with dimensions that exceed the limit by diffusive transport alone.

The development of large three-dimensional engineered tissue constructs requires convective transport of nutrients to the inner part of the tissue quickly after implantation. Incorporation of ECs in tissue constructs has been demonstrated to be an effective method to develop vessel networks. For example, robust vessel networks were formed by transplantation of ECs transduced with the *bcl-2* gene[28] or human telomerase reverse transcriptase,[29] or the cotransplantation of ECs with stromal cells in a gel matrix.[11,17–19] These tissues supported generation of vessels *in vivo* that anastomosed with the host vasculature, showed structural and functional properties mimicking native vessels,[11,30] and were functional for up to 60 days after transplantation. However, the time required for the formation of functional vessel networks was relatively long (7–14 days), which may not be adequate for oxygen-sensitive cells (e.g., cardiomyocytes).

In our previous study,[23] we demonstrated that prevascularization of the engineered tissue constructs with well-formed vessel networks before implantation accelerated the development of functional anastomosis with the host vasculature (5–7 days for the prevascularized tissue constructs vs. 7–14 days for tissue constructs seeded with ECs and fibroblasts but not allowed to form vessel networks before implantation). In this study, we aimed to further reduce the time for the development of functional anastomosis. By increasing the seeding density of fibroblasts and using cord blood EPC-ECs instead of HUVECs, the preformed vessels demonstrated anastomosis with the host vasculature as early as 1 day (27 h) postimplant, and most of the tissue constructs (six out of seven) were perfused by day 3. The perfusion of implanted tissues by host blood in such a short time will likely alleviate postimplant tissue hypoxia and promote the survival of cells in the inner portion of larger tissue constructs.

EPCs are derived from the bone marrow, and migrate into the systemic circulation in response to a variety of signal molecules, such as vascular endothelial growth factor, released by ischemic tissues or damaged vessels.[31] The circulating EPCs migrate to the sites of hypoxia or injured vessels, and incorporate into the sprouting neovessels or participate in the re-endothelialization of damaged vessels. Since the initial reports of separating EPCs from peripheral blood,[32] circulating EPCs have been isolated with antibodies specific to a variety of cell surface markers, including the progenitor/stem cell marker CD133,[33] the endothelial marker CD34,[32,34,35] CD31,[18,24] or a combination of endothelial and progenitor cell markers.[36] In this study, we purified the endothelial outgrowth of CD31-positive cells from cord blood, but EPCs derived from adult blood have also been shown to have equivalent angiogenic potential when implanted with bone marrow mesenchymal cells.[18,24] The EPC-ECs in our study showed similar morphology and high (relative to HUVECs) *in vitro* expansion capacity consistent with previous reports.[24] The superior angiogenic potential of EPC-ECs both *in vitro* and *in vivo* compared to HUVECs may be related to the higher *in vitro* proliferation rate. We also demonstrated that EPC-ECs were more sensitive to proangiogenic molecules produced by fibroblasts (Fig. 1E, F), which may also contribute to the superior *in vitro* and *in vivo* performance. Finally, the seeding density of HUVECs and EPC-ECs (1 million/mL) was chosen based on our previous study.[23] A higher density of HUVECs compromised the development of vessels, most likely due to the limited supply of nutrients and proangiogenic molecules in the tissue construct.

In our previous study, we demonstrated that the presence of fibroblasts is critical for the formation of vessel networks *in vitro*.[23] The 1:5 ratio of fibroblasts to ECs used in our previous study was based on previous reports in the literature.[6,12] However, the recent work by Melero-Martin *et al.*[18] indicated that a higher density of fibroblasts promoted the *in vivo* formation of vessels by transplanted EPCs. In our current study, we increased the density of fibroblasts from 0.2 to 2 million cells/mL (thus, the ratio of fibroblasts to ECs increased from 1:5 to 2:1) and observed enhanced formation

of vessel networks *in vitro*, and accelerated anastomosis with host vasculature *in vivo*. The mechanism for the improved performance of the vessel network in the presence of a higher concentration of fibroblast may be the result of several factors. For example, soluble angiogenic molecules are produced by the fibroblasts,[25,26] and a higher concentration of fibroblasts may result in a higher concentration of proangiogenic molecules. Additionally, the higher concentration of fibroblasts will consume more oxygen and may create a locally hypoxic environment that favors the production of proangiogenic factors. Fibroblasts are also involved in the remodeling of extracellular matrix proteins[37] through the production of matrix metalloproteinases,[38] as well as the stabilization of the newly formed vessels by the association of myofibroblasts or pericytes.[23] Interestingly, we previously demonstrated that the fibroblasts in these cultures rapidly (by day 3) assume a myofibroblast phenotype, as evidenced by their expression of α-SMA and fibronectin containing the extra domain A splice variant, an inducer of myofibroblast differentiation.[18,26] Further, in our current study, we observed α-SMA–positive cells wrapped around the vessels formed by HUVECs or EPC-ECs, but to a greater degree with EPC-EC–derived vessels (Fig. 6). The enhanced pericyte-like behavior by the fibroblasts may contribute to enhanced vessel formation *in vitro* and *in vivo*.

In summary, we have developed an interconnected, three-dimensional network of mature capillaries (i.e., capillaries enveloped by pericyte-like support cells) that can connect to the host vasculature as early as 1 day after implantation. The tissue constructs comprised of EPC-ECs and a high density of fibroblasts not only promoted the development of vessel networks *in vitro*, but also accelerated the rate of anastomosis *in vivo*. Our results demonstrate the promise of prevascularizing an implantable tissue construct and the suitability of EPC-ECs as the source of ECs. Future work must address the potential of this approach in larger (i.e., dimensions >1 cm) tissues as a means of enhancing tissue survival after implantation.

Acknowledgments

We acknowledge the assistance of Dr. Christopher Raub in the imaging of the *in vitro* vessels with the confocal microscope. We would also like to thank Mr. Danny Spampinato and Mr. Travis Kruse for their assistance in quantifying the *in vitro* and *in vivo* vascular networks. This work was supported in part by grants from the National Institutes of Health (R01 HL067954 [S.C.G.] and R01 HL086959 [C.C.W.H.]), as well as the Whitaker Foundation, and the multiinvestigator research grants from the Committee on Research and Library Resources from the University of California–Irvine.

Disclosure Statement

No competing financial interests exist.

References

1. Langer, R., and Vacanti, J.P. Tissue engineering. Science **260,** 920, 1993.
2. Vacanti, J.P., and Langer, R. Tissue engineering: the design and fabrication of living replacement devices for surgical reconstruction and transplantation. Lancet **354 Suppl 1,** SI32, 1999.
3. Falabella, A.F., Schachner, L.A., Valencia, I.C., and Eaglstein, W.H. The use of tissue-engineered skin (Apligraf) to treat a newborn with epidermolysis bullosa. Arch Dermatol **135,** 1219, 1999.
4. Ando, W., Tateishi, K., Hart, D.A., Katakai, D., Tanaka, Y., Nakata, K., Hashimoto, J., Fujie, H., Shino, K., Yoshikawa, H., and Nakamura, N. Cartilage repair using an *in vitro* generated scaffold-free tissue-engineered construct derived from porcine synovial mesenchymal stem cells. Biomaterials **28,** 5462, 2007.
5. Kang, P.M., Haunstetter, A., Aoki, H., Usheva, A., and Izumo, S. Morphological and molecular characterization of adult cardiomyocyte apoptosis during hypoxia and reoxygenation. Circ Res **87,** 118, 2000.
6. Laflamme, M.A., Chen, K.Y., Naumova, A.V., Muskheli, V., Fugate, J.A., Dupras, S.K., Reinecke, H., Xu, C., Hassanipour, M., Police, S., O'Sullivan, C., Collins, L., Chen, Y., Minami, E., Gill, E.A., Ueno, S., Yuan, C., Gold, J., and Murry, C.E. Cardiomyocytes derived from human embryonic stem cells in pro-survival factors enhance function of infarcted rat hearts. Nat Biotechnol **25,** 1015, 2007.
7. Tremblay, P.L., Hudon, V., Berthod, F., Germain, L., and Auger, F.A. Inosculation of tissue-engineered capillaries with the host's vasculature in a reconstructed skin transplanted on mice. Am J Transplant **5,** 1002, 2005.
8. Levenberg, S., Rouwkema, J., Macdonald, M., Garfein, E.S., Kohane, D.S., Darland, D.C., Marini, R., van Blitterswijk, C.A., Mulligan, R.C., D'Amore, P.A., and Langer, R. Engineering vascularized skeletal muscle tissue. Nat Biotechnol **23,** 879, 2005.
9. Caspi, O., Lesman, A., Basevitch, Y., Gepstein, A., Arbel, G., Habib, I.H., Gepstein, L., and Levenberg, S. Tissue engineering of vascularized cardiac muscle from human embryonic stem cells. Circ Res **100,** 263, 2007.
10. Jain, R.K., Au, P., Tam, J., Duda, D.G., and Fukumura, D. Engineering vascularized tissue. Nat Biotechnol **23,** 821, 2005.
11. Koike, N., Fukumura, D., Gralla, O., Au, P., Schechner, J.S., and Jain, R.K. Tissue engineering: creation of long-lasting blood vessels. Nature **428,** 138, 2004.
12. Black, A.F., Berthod, F., L'Heureux, N., Germain, L., and Auger, F.A. *In vitro* reconstruction of a human capillary-like network in a tissue-engineered skin equivalent. FASEB J **12,** 1331, 1998.
13. Nor, J.E., Peters, M.C., Christensen, J.B., Sutorik, M.M., Linn, S., Khan, M.K., Addison, C.L., Mooney, D.J., and Polverini, P.J. Engineering and characterization of functional human microvessels in immunodeficient mice. Lab Invest **81,** 453, 2001.
14. Ferreira, L.S., Gerecht, S., Shieh, H.F., Watson, N., Rupnick, M.A., Dallabrida, S.M., Vunjak-Novakovic, G., and Langer, R. Vascular progenitor cells isolated from human embryonic stem cells give rise to endothelial and smooth muscle like cells and form vascular networks *in vivo*. Circ Res **101,** 286, 2007.
15. McCloskey, K.E., Gilroy, M.E., and Nerem, R.M. Use of embryonic stem cell-derived endothelial cells as a cell source to generate vessel structures *in vitro*. Tissue Eng **11,** 497, 2005.
16. Drukker, M., Katchman, H., Katz, G., Even-Tov Friedman, S., Shezen, E., Hornstein, E., Mandelboim, O., Reisner, Y., and Benvenisty, N. Human embryonic stem cells and their differentiated derivatives are less susceptible to immune rejection than adult cells. Stem Cells **24,** 221, 2006.

17. Traktuev, D.O., Prater, D.N., Merfeld-Clauss, S., Sanjeevaiah, A.R., Murphy, M., Johnstone, B.H., Ingram, D.A., and March, K.L. Robust functional vascular network formation *in vivo* by cooperation of adipose progenitor and endothelial cells. Circ Res **104,** 1410, 2009.
18. Melero-Martin, J.M., De Obaldia, M.E., Kang, S.Y., Khan, Z.A., Yuan, L., Oettgen, P., and Bischoff, J. Engineering robust and functional vascular networks *in vivo* with human adult and cord blood-derived progenitor cells. Circ Res **103,** 194, 2008.
19. Au, P., Daheron, L.M., Duda, D.G., Cohen, K.S., Tyrrell, J.A., Lanning, R.M., Fukumura, D., Scadden, D.T., and Jain, R.K. Differential *in vivo* potential of endothelial progenitor cells from human umbilical cord blood and adult peripheral blood to form functional long-lasting vessels. Blood **111,** 1302, 2008.
20. Ingram, D.A., Mead, L.E., Tanaka, H., Meade, V., Fenoglio, A., Mortell, K., Pollok, K., Ferkowicz, M.J., Gilley, D., and Yoder, M.C. Identification of a novel hierarchy of endothelial progenitor cells using human peripheral and umbilical cord blood. Blood **104,** 2752, 2004.
21. Chade, A.R., Zhu, X., Lavi, R., Krier, J.D., Pislaru, S., Simari, R.D., Napoli, C., Lerman, A., and Lerman, L.O. Endothelial progenitor cells restore renal function in chronic experimental renovascular disease. Circulation **119,** 547, 2009.
22. Nagano, M., Yamashita, T., Hamada, H., Ohneda, K., Kimura, K., Nakagawa, T., Shibuya, M., Yoshikawa, H., and Ohneda, O. Identification of functional endothelial progenitor cells suitable for the treatment of ischemic tissue using human umbilical cord blood. Blood **110,** 151, 2007.
23. Chen, X., Aledia, A.S., Ghajar, C.M., Griffith, C.K., Putnam, A.J., Hughes, C.C., and George, S.C. Prevascularization of a fibrin-based tissue construct accelerates the formation of functional anastomosis with host vasculature. Tissue Eng Part A **15,** 1363, 2009.
24. Melero-Martin, J.M., Khan, Z.A., Picard, A., Wu, X., Paruchuri, S., and Bischoff, J. *In vivo* vasculogenic potential of human blood-derived endothelial progenitor cells. Blood **109,** 4761, 2007.
25. Griffith, C.K., Miller, C., Sainson, R.C., Calvert, J.W., Jeon, N.L., Hughes, C.C., and George, S.C. Diffusion limits of an *in vitro* thick prevascularized tissue. Tissue Eng **11,** 257, 2005.
26. Ghajar, C.M., Chen, X., Harris, J.W., Suresh, V., Hughes, C.C., Jeon, N.L., Putnam, A.J., and George, S.C. The effect of matrix density on the regulation of 3-D capillary morphogenesis. Biophys J **94,** 1930, 2008.
27. Nakatsu, M.N., Sainson, R.C., Aoto, J.N., Taylor, K.L., Aitkenhead, M., Perez-del-Pulgar, S., Carpenter, P.M., and Hughes, C.C. Angiogenic sprouting and capillary lumen formation modeled by human umbilical vein endothelial cells (HUVEC) in fibrin gels: the role of fibroblasts and angiopoietin-1. Microvasc Res **66,** 102, 2003.
28. Schechner, J.S., Nath, A.K., Zheng, L., Kluger, M.S., Hughes, C.C., Sierra-Honigmann, M.R., Lorber, M.I., Tellides, G., Kashgarian, M., Bothwell, A.L., and Pober, J.S. *In vivo* formation of complex microvessels lined by human endothelial cells in an immunodeficient mouse. Proc Natl Acad Sci USA **97,** 9191, 2000.
29. Yang, J., Nagavarapu, U., Relloma, K., Sjaastad, M.D., Moss, W.C., Passaniti, A., and Herron, G.S. Telomerized human microvasculature is functional *in vivo*. Nat Biotechnol **19,** 219, 2001.
30. Enis, D.R., Shepherd, B.R., Wang, Y., Qasim, A., Shanahan, C.M., Weissberg, P.L., Kashgarian, M., Pober, J.S., and Schechner, J.S. Induction, differentiation, and remodeling of blood vessels after transplantation of Bcl-2-transduced endothelial cells. Proc Natl Acad Sci USA **102,** 425, 2005.
31. Hristov, M., Erl, W., and Weber, P.C. Endothelial progenitor cells: mobilization, differentiation, and homing. Arterioscler Thromb Vasc Biol **23,** 1185, 2003.
32. Asahara, T., Murohara, T., Sullivan, A., Silver, M., van der Zee, R., Li, T., Witzenbichler, B., Schatteman, G., and Isner, J.M. Isolation of putative progenitor endothelial cells for angiogenesis. Science **275,** 964, 1997.
33. Quirici, N., Soligo, D., Caneva, L., Servida, F., Bossolasco, P., and Deliliers, G.L. Differentiation and expansion of endothelial cells from human bone marrow CD133(+) cells. Br J Haematol **115,** 186, 2001.
34. Zhu, C., Ying, D., Mi, J., Li, L., Zeng, W., Hou, C., Sun, J., Yuan, W., Wen, C., and Zhang, W. Development of anti-atherosclerotic tissue-engineered blood vessel by A20-regulated endothelial progenitor cells seeding decellularized vascular matrix. Biomaterials **29,** 2628, 2008.
35. Droetto, S., Viale, A., Primo, L., Jordaney, N., Bruno, S., Pagano, M., Piacibello, W., Bussolino, F., and Aglietta, M. Vasculogenic potential of long term repopulating cord blood progenitors. FASEB J **18,** 1273, 2004.
36. Khan, Z.A., Melero-Martin, J.M., Wu, X., Paruchuri, S., Boscolo, E., Mulliken, J.B., and Bischoff, J. Endothelial progenitor cells from infantile hemangioma and umbilical cord blood display unique cellular responses to endostatin. Blood **108,** 915, 2006.
37. Ghajar, C.M., Blevins, K.S., Hughes, C.C., George, S.C., and Putnam, A.J. Mesenchymal stem cells enhance angiogenesis in mechanically viable prevascularized tissues via early matrix metalloproteinase upregulation. Tissue Eng **12,** 2875, 2006.
38. Ghajar, C.M., George, S.C., and Putnam, A.J. Matrix metalloproteinase control of capillary morphogenesis. Crit Rev Eukaryot Gene Expr **18,** 251, 2008.

Address correspondence to:
Steven C. George, M.D., Ph.D.
Department of Biomedical Engineering
University of California, Irvine
2420 Engineering Hall
Irvine, CA 92697-2730

E-mail: scgeorge@uci.edu

Received: July 16, 2009
Accepted: September 3, 2009
Online Publication Date: November 6, 2009